

Claremont Colleges

Scholarship @ Claremont

HMC Senior Theses

HMC Student Scholarship

2007

An ODE Model of Biochemotherapy Treatment for Cancer

James Moore
Harvey Mudd College

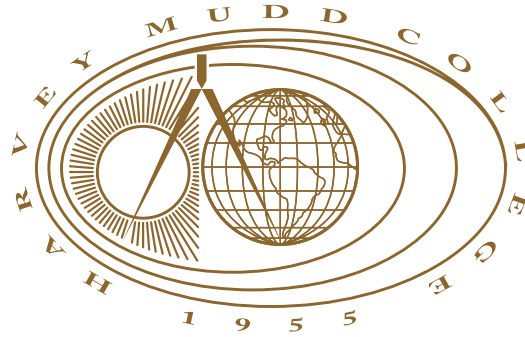
Follow this and additional works at: https://scholarship.claremont.edu/hmc_theses

Recommended Citation

Moore, James, "An ODE Model of Biochemotherapy Treatment for Cancer" (2007). *HMC Senior Theses*. 200.

https://scholarship.claremont.edu/hmc_theses/200

This Open Access Senior Thesis is brought to you for free and open access by the HMC Student Scholarship at Scholarship @ Claremont. It has been accepted for inclusion in HMC Senior Theses by an authorized administrator of Scholarship @ Claremont. For more information, please contact scholarship@claremont.edu.



An ODE Model of Biochemotherapy Treatment for Cancer

James Moore

Jon Jacobsen, Advisor

Lisette de Pillis, Reader

May, 2007

HARVEY MUDD
COLLEGE

Department of Mathematics

Copyright © 2007 James Moore.

The author grants Harvey Mudd College the nonexclusive right to make this work available for noncommercial, educational purposes, provided that this copyright statement appears on the reproduced materials and notice is given that the copying is by permission of the author. To disseminate otherwise or to republish requires written permission from the author.

Abstract

Cancer is one of the most prevalent and deadly diseases in the United States today. There are many approaches to treating cancer, but here we focus on biochemotherapy which is a combination of chemotherapy and immunotherapy. The intent of immunotherapy is to boost the body's natural resistance to cancer which is often repressed by the regulatory branch of the immune system. Here we show that this repression may be overcome by chemotherapy followed closely by immunotherapy. However, giving immunotherapy at the wrong time can actually promote tumor growth.

Contents

Abstract	iii
Acknowledgments	xi
1 Introduction	1
1.1 Cancer	1
1.2 Approaches to Modeling Cancer	1
1.3 Immune Response	2
1.4 Cancer Treatment	3
2 Biology Overview	5
2.1 Immunity and Tolerance	5
2.2 The role of IL-2	5
2.3 Tregs and Dendritic Cells	6
2.4 The role of IL-10	6
3 Prior Mathematical Models	7
3.1 Kirschner and Panetta, 1997	7
3.2 Depillis et al. 2006	8
4 New Model Formulation	11
4.1 Immune Responsiveness Functions	12
4.2 Dendritic Cells	12
4.3 Cytotoxic T-Cells	12
4.4 Regulatory T-Cells	13
4.5 Cytokines	13
4.6 Tumor Dynamics	14
4.7 Chemotherapy	14
4.8 The Model	15

5	Mathematical Background	17
5.1	Linear Stability Analysis	17
5.2	Phase Plane Analysis	18
5.3	Seperation of Time Scales	22
6	Infection-Free Dynamics	25
6.1	Derivation of the Reduced Model	25
6.2	Analysis	26
6.3	Limit Cycle	30
7	Adapting the Model	33
7.1	Removal of Naive T-Cell Population	33
7.2	Seperating the Cytokine Time Scale	33
7.3	Removal of Dendritic Cell Populations	34
8	Analyzing the new Model	37
9	Conclusion	45
9.1	Lessons From the Model	45
9.2	Future Work	46
	Bibliography	49
A	Parameters	53
B	Non-Dimensionalization	57
B.1	Parameters	58

List of Figures

5.1	Behavior in One Dimension	18
5.2	Bifurcations	20
5.3	Phase Plane Analysis	21
6.1	Limit Cycle	31
8.1	Fast Time Scale	38
8.2	Surface of the slow timescale	39
8.3	Regions of State Space	41
8.4	Phase plot of slow time scale	42

List of Tables

A.1	Death and Decay Rates	53
A.2	Other Growth Rates	53
A.3	Other Growth and Death Rates	54
A.4	Source, Activation and Deactivation Terms	54
A.5	Levels of Half-Maximal Activation	54
A.6	Potential Fits to Data	55
A.7	Parameters of the Reduced System	55
B.1	Parameters of Non-Dimensionalized Model	58

Acknowledgments

I'd like to thank my advisor, Jon Jacobsen, for his guidance throughout this project. I'd also like to thank Professors Lisette de Pillis and Weiqing Gu, who got me interested in this problem. Finally, I'd like to recognize David Gross '08, Ben Preskill '09, and Michael Daub (Williams '09) who worked with me over the summer and the HMC Math and Biology Departments for giving me the necessary skills to undertake this project.

Chapter 1

Introduction

1.1 Cancer

In the United States alone, there are more than one million new cases of cancer reported each year [25]. More than 1 in 3 people who live to age 90 will get cancer at some point in their lives [25]. Cancer is the unchecked proliferation of a cell inside the body. The rapidly dividing cells will usually not perform their function correctly and instead impede the action of their neighbors. This often leads to death; an estimated half a million people will die of cancer in the US this year [25].

As a tumor grows, it requires more nutrients to feed itself. Nutrients must diffuse through surrounding tissue, and so the center of the tumor becomes a **necrotic core**, or mass of dead tissue. Sometimes, tumors can promote **angiogenesis**, the growth of new blood vessels. The new blood supply allows the tumor to grow larger and spread to other tissues (**metastasis**). In this paper, we do not consider angiogenesis or metastasis, but rather a tumor limited by nutrient diffusion. Our goal is to find ways to treat tumors before they can reach such an advanced stage of development.

1.2 Approaches to Modeling Cancer

Models of cancer vary in both their focus and mathematical approach. Many models have been developed to take into account the logistics of a growing tumor. These include nutrient uptake, **vascularization** (the process by which tumors acquire a blood supply), and metastasis [3]. This paper will focus on the interaction of the immune system with cancer and the effect that treatment has on that interaction.

Fundamentally, the model is a system of ordinary differential equation or **ODEs**. Such a system has the form.

$$\frac{d}{dt}\vec{X}(t) = \vec{f}(\vec{X}(t)), \quad (1.1)$$

where $\vec{X}(t)$ is the **state variable**, whose trajectory is dependent upon the **vector field**, \vec{f} . The components of $\vec{X}(t)$ consist of important quantities that dynamically change in time, such as various cell or drug concentrations and the vector \vec{f} describes the interaction between these quantities. An ODE model assumes that the body is a well-mixed system with no spatial heterogeneity. It is also completely deterministic as opposed to a stochastic model. Modeling approaches that include spatial structure are partial differential equations and cellular automata. Both have been used in the context of cancer modeling (see [11] for PDEs and [20] for cellular automata). In a partial differential equation, the state variable is a function of more than one independent variable, often space and time. This allows for simple models of nutrient diffusion [3] as well as complex models of blood vessel growth [16]. In a cellular automata, each cell is modeled individually and changes its own state based upon the state of the cells adjacent to it. These approaches can also be combined, as in [18], where a cellular automata model governs the state of each cell, but the dynamics of nutrient concentrations are governed by a partial differential equation.

1.3 Immune Response

The human immune system consists of a variety of specialized cells designed to respond in different ways to different types of invaders. Here we focus on the **cellular response**, the creation of a population of cells known as **T-cells** to combat a specific invader. The immune system can normally detect the presence of abnormal cells due to changes in the proteins expressed on their surface. These proteins, known as **antigens**, are recognized by the body as either self-antigens or foreign antigens. Normal cells in the body express self-antigens, whereas invading bacteria or cells that have been infected by a virus express foreign antigens. Once an antigen is recognized, the immune system promotes the proliferation of the antigen-specific T-cells.

T-cells which do not yet have the ability to kill other cells are called **naive** T-cells. They become **cytotoxic**, capable of killing other cells, upon

stimulation by an **APC** or antigen presenting cell. T-cells respond to specific antigens, so they can only be activated by certain antigen presenting cells. Those that respond to self-antigens are deleted. Tumors cells are dysfunctional, not invasive, which means that they may or may not express foreign antigens. Therefore, the cells which respond to the tumor might be deleted. This can create difficulties in cancer treatment, because the body may suppress its natural defense against tumor growth. A response can also be prevented directly by the action of the tumor, through the release of certain chemicals and the direct deletion of immune cells (see [29] and [19] for a review of the ways in which tumors evade the immune system).

1.4 Cancer Treatment

There are many possible approaches to treating cancer. One popular approach is **cytotoxic chemotherapy**: the administration of a drug designed to kill rapidly dividing cells. Although it is often effective, it harms normal tissues as well as cancerous ones and therefore has many unpleasant side effects. An alternative approach is **immunotherapy**, which is a general term for any treatment aimed to improve the bodies own immune response. The use of immunotherapy in conjunction with cytotoxic chemotherapy is known as **biochemotherapy**. Other treatment options include **radiation therapy** and surgery, which try to kill or remove the tissue that contains the tumor. In this paper, we will focus on biochemotherapy treatment using the immunological drug Interleukin-2, referred to from now on as **IL-2**. Current biochemotherapy schedules have unpredictable success [2]. These clinical results may perhaps be due to the complex action of IL-2, as described below, which immunologists claim requires a reexamination of cancer treatment [21]. The aim of this thesis is to model the interaction of chemotherapy and immunotherapy to create more effective biochemotherapy treatments.

Chapter 2

Biology Overview

2.1 Immunity and Tolerance

From our standpoint, the goal of the immune system should be to maximize the number of immune cells that are primed to kill tumor cells. The primary difficulty for the immune system, however, is maintaining the balance between immunity and tolerance (see [21], [28], [4], [1]). On the one hand, the immune system could err on the side of immunity and start to attack cells within the body indiscriminately. This is called **autoimmunity** and can be quite serious. On the other hand, the immune system could err on the side of tolerance, ignoring cells which are actually harmful to the body. In general, the immune system relies upon antigens to distinguish between cells “self” and “nonself”. Each T-cell, however, does not contain a catalog of which antigens are foreign; they each have a specific target and kill it whenever they find it. Leon et al. ([4], [15]) have written several papers modeling immune tolerance. Their goal was to test hypothesized mechanisms of immune regulation. Although subsequent experiments have made their research somewhat obsolete, they demonstrated the plausibility of immune tolerance as an emergent behavior of the immune system. Here we introduce and discuss the important processes in the regulation of immunity and tolerance.

2.2 The role of IL-2

IL-2, a naturally produced molecule, is a widely administered immunotherapy drug, particularly for cancer. The activity of this molecule is often included in immunological models of cancer treatment (see e.g. [6],[7],[14]).

In these models, it is assumed that IL-2 is a growth factor for T-cells. More recent research has shown that IL-2 may work in far more complex ways than previously thought ([24],[21]). Antigen-stimulated T-cells become sensitive to activation-induced cell death upon stimulation by IL-2 [24]. That is to say that once activated by an APC, the T-cell may be deleted if it is activated again by an APC. This means that although IL-2 promotes the proliferation of T-cells, it also shortens their lifespan.

It is now thought that the most important role of IL-2 is in the maintenance of immune tolerance as mediated by regulatory T-cells or **Tregs** [21]. IL-2 is vital for the proliferative expansion of these cells [21]. These cells are produced in response to chronic antigen stimulation to protect against possible autoimmunity. Tregs act upon cytotoxic T-cells by preventing the latter cell type from producing IL-2, thus preventing their proliferation (see [27],[22]). The size of the Treg and IL-2 producing T cell subsets has been shown to correlate, indicating a likely negative feedback [1].

2.3 Tregs and Dendritic Cells

A basic principle of immunology is that T-cells must be activated by contact with an APC. The most important type of APC are known as **dendritic cells**. Tregs can modify the function of dendritic cells by making them **tolerogenic** [28]. These tolerogenic dendritic cells deactivate cytotoxic T-cells [28] and cause the creation of new Tregs from certain naive T-cells [28].

2.4 The role of IL-10

Another cytokine, Interleukin-10, plays an important role in both processes mentioned above. First, Tregs act upon cytotoxic T-cells through the release of IL-10 ([28]). Second, dendritic cells can induce a subset of T-cell to produce IL-10 ([28]). Finally, IL-10 can cause some dendritic cells to become tolerogenic ([28]).

Chapter 3

Prior Mathematical Models

Due to the relatively recent discovery of the immunological processes involved, few mathematical models exist for them. Despite the large number of papers modeling cancer (for a general review see [3]), no model currently exists that combines:

- A growing tumor
- Regulatory T-cells
- Dendritic cells
- Interleukin-2
- Chemotherapy

The following papers have addressed one or more of the above components and are of interest to us.

3.1 Kirschner and Panetta, 1997

In [14], Kirschner and Panetta consider a 3-dimensional ODE that takes into account the basic attributes of IL-2:

$$\begin{aligned}\frac{dE}{dt} &= cT - \mu_2 E + \frac{p_1 E I_L}{g_1 + I_L} + s_1 \\ \frac{dT}{dt} &= r_2(1 - bT)T - \frac{aET}{g_2 + T} \\ \frac{dI_L}{dt} &= \frac{p_2 ET}{g_3 + T} - \mu_3 I_L + s_2.\end{aligned}$$

In their model, E represents the number of effector (we would say cytotoxic) cells, T is the number tumor cells and I_L is the concentration of IL-2. They assume that IL-2 acts as a simple growth factor for IL-2. Although this is true, this is not what is considered the most immunologically relevant action of IL-2, as mentioned in §2.2. The variables s_1 and s_2 represent outside input from treatment, either in the form of primed effector cells (s_1) or IL-2 (s_2). By adding enough effector cells through s_1 , the population E can be made arbitrarily large, killing the tumor. However, we know that the immune system's own self-regulation can keep the level of effector cells below what is required to kill the tumor [19]. Thus, it seems that a new model is necessary in order to take this into account.

3.2 Depillis et al. 2006

In a series of unpublished papers de Pillis et al. [5] develop and analyze a model of IL-2 treatment, chemotherapy, adoptive cell transfer therapy, and the tumor-immune interaction. In their ODE model, cytotoxic T-cells are represented as a single population of uniform cells. Tregs are assumed to be a subset of another population, circulating lymphocytes. Their model assumes:

- The level of circulating lymphocytes is proportional to T-cell deactivation or apoptosis;
- IL-2 is necessary for the regulation of cytotoxic T-cells by circulating lymphocytes;
- IL-2 reduces the “natural” death rate of T-cells;
- T-cells produce IL-2 upon activation;
- Circulating lymphocytes produce IL-2 at a constant low level;
- IL-2 causes T-cells to divide and proliferate.

All of these assumptions are incorporated into 2 ODEs:

$$\begin{aligned}\frac{dT}{dt} &= -\frac{mT}{1+I} + rT + \frac{jT}{k+T} - qLT + (p_I - u_0L)\frac{IL}{1+I} \\ \frac{dI}{dt} &= \phi - \mu_I I + \frac{\omega I}{1+I}\end{aligned}$$

where L is the number of T-cells and I is the amount of IL-2. Analysis of the whole model shows that chemotherapy is very important in the treatment of cancer. It removed regulatory T-cells and allowed for a huge increase in cytotoxic T-cells. However, the model also makes the following assumptions:

- Antigen stimulated T-cells are all alike;
- Antigen stimulation plays no role in regulation;
- Tregs are a constant proportion of circulating lymphocytes.

Given the important role that regulatory T-cells had in the treatment of cancer, it seems vital that they be considered as a separate population. Also, antigen stimulation and IL-2 have opposite effects on classes of T-cells which were lumped together under this model. Thus, a more thorough treatment of the T-cell dynamics is necessary.

Chapter 4

New Model Formulation

Based on the new immunological findings and lessons learned from previous models, we propose a new model. This model incorporates dendritic cells, cytotoxic T-cells, Tregs and the two cytokines: IL-2 and IL-10. All cell populations are assumed to be antigen specific. The following variables will stand for important species:

- $D_I(t)$ Immature dendritic cells
- $D(t)$ Immunogenic dendritic cells
- $D_T(t)$ Tolerogenic dendritic cells
- $T_N(t)$ Naive T-cells
- $T_C(t)$ Cytotoxic T-cells
- $T_{CP}(t)$ Proliferating cytotoxic T-cells
- $T_R(t)$ Regulatory T-cells
- $I_2(t)$ Interleukin 2 (IL-2)
- $I_{10}(t)$ Interleukin 10 (IL-10)
- $C(t)$ Cancer cells
- $M(t)$ Chemotherapy medicine

4.1 Immune Responsiveness Functions

We will also consider the functions $A_i = A(C)$ ($i = 1..3$) which model the stimulation of the immune system at various tumor sizes. The first function A_1 is the rate at which new dendritic cells primed against a particular antigen are created. The function A_2 is the rate at which APCs other than dendritic cells activate cytotoxic T-cells. Finally, A_3 is the rate at which cytotoxic T-cells are deleted through overstimulation. We assume that each of these functions increases monotonically. We assume $A_i(0) > 0$ for self antigens and $A_i(0) = 0$ for foreign antigens.

4.2 Dendritic Cells

As mentioned above, we assume that new immature dendritic cells, D_I , are formed at a rate A_1 , which is dependent upon tumor size, C . They either mature into immunogenic dendritic cells, D , or, should they interact with either IL-10, I_{10} , or a Treg, T_R , into a tolerogenic dendritic cell, D_T . All three populations also have linear natural death terms. This yields three equations:

$$\frac{dD_I}{dt} = A_1(C) - aD_I - a_T D_I \frac{T_R}{g_R + T_R} - \omega_I D_I - b_T D_I \frac{I_{10}}{g_{10} + I_{10}} \quad (4.1)$$

$$\frac{dD}{dt} = aD_I - \omega D \quad (4.2)$$

$$\frac{dD_T}{dt} = a_T D_I \frac{T_R}{g_R + T_R} + b_T D_I \frac{I_{10}}{g_{10} + I_{10}} - \omega_T D_T. \quad (4.3)$$

4.3 Cytotoxic T-Cells

The cytotoxic T-cells, T_C , derive from the naive T-cell population, T_N . The size of this source population depends upon IL-2 indirectly. Unactivated T-cells are subject to "death by neglect", a process that is prevented by IL-2. We assume that naive T-cells are created at a constant rate (α_N) and die at a rate dependent on I_2 . Naive T-cells become activated by antigen presenting cells, APCs. Non-dendritic cell APCs activate naive T-cells at a rate $A_2(C)$. Interaction of a tolerogenic dendritic cell and a cytotoxic T-cell leads to nonresponsiveness at a rate d . This process is treated the same way as death, as the T-cell no longer fulfills its function ([26]). In addition, this population of cells has a natural death rate, ω_C .

The cytotoxic cells become proliferative upon interaction with IL-2 at a rate, a_{CP} . They become non-proliferative at a rate d_{CP} upon interaction with IL-10. Both of these processes plateau at high levels of the cytokines as in prior models of cytokine activity [14]. Proliferating cells also have an intrinsic growth rate γ . The proliferating cells are inactivated through repeated antigen stimulation at a rate $A_3(C)$. This yields three more equations:

$$\frac{dT_N}{dt} = \alpha_N - \frac{\omega_N}{g_2 + I_2} T_N \quad (4.4)$$

$$\begin{aligned} \frac{dT_C}{dt} &= a_C T_N D + T_N A_2(C) - d_{D_T} T_C - a_{CP} T_C \frac{I_2}{g_2 + I_2} \\ &+ d_{CP} T_{CP} \frac{I_{10}}{g_{10} + I_{10}} - \omega_C T_C \end{aligned} \quad (4.5)$$

$$\frac{dT_{CP}}{dt} = a_{CP} T_C \frac{I_2}{g_2 + I_2} - d_{CP} T_C \frac{I_{10}}{g_{10} + I_{10}} + \gamma T_{CP} - A_3(C). \quad (4.6)$$

4.4 Regulatory T-Cells

Regulatory T-cells, T_R , differentiate from the Naive T-cell population upon interaction with a tolerogenic dendritic cell at a rate a_R . Interaction with IL-2 causes the regulatory T-cells to expand at a rate c . Like all other terms involving IL-2, its value plateaus. Finally, the Tregs have a natural death rate, ω_R . This yields:

$$\frac{dT_R}{dt} = a_R D_T T_N + c T_R \frac{I_2}{n + I_2} - \omega_R T_R. \quad (4.7)$$

Unlike for the cytotoxic T-cells, we do not create separate populations for proliferating and non-proliferating regulatory T-cells. The cytotoxic T-cells warranted two separate equations because different types of cytotoxic T-cells respond to regulatory T-cells and APCs in opposing manners. This is not the case for Tregs, so we find one equation sufficient.

4.5 Cytokines

We assume IL-2 is produced at a constant rate by naive T-cells. It also decays at a constant rate ω_2 . The interaction of a cytotoxic T-cell with IL-2 causes the T-cell to release IL-2 at a rate a_2 [5]. The interaction of naive $CD4^+$ T-cells with immature dendritic cells causes them to release IL-10

[28]. We model this by assuming that IL-10 production is proportional to D_I . Treg-CTL interaction also induces the production of IL-10 at a rate a_{10} . The decay rate for IL-10 is ω_{10} . This yields:

$$\frac{dI_2}{dt} = \alpha_2 T_N - \omega_2 I_2 + a_2 T_c \frac{I_2}{n + I_2} \quad (4.8)$$

$$\frac{dI_{10}}{dt} = \alpha_{10} D_I + a_{10} T_R T_c - \omega_{10} I_{10}. \quad (4.9)$$

4.6 Tumor Dynamics

The interaction of the tumor with the immune system is mainly via cytotoxic T-cells. The rate at which cytotoxic cells kill tumor cells has been modeled [6] as

$$D_C = d \frac{(L/C)^l}{s + (L/C)^l}$$

where C is the size of the tumor and $T = T_c + T_{CP}$. In [6], it is assumed that the tumor grows logistically.

$$\frac{dC}{dt} = fC(1 - hC) - D_C C, \quad (4.10)$$

which is accurate for non-vascularized tumors (see [3] for other possible growth functions).

4.7 Chemotherapy

As in [6], we may model chemotherapy by adding on a term of the form $k_X X(1 - e^{\delta_X M})$ to $\frac{dX}{dt}$ where X can be any cell already modeled and M is the concentration of the chemotherapy drug ([12]). We assume that the chemotherapy drug decays at a rate ω_M :

$$\frac{dM}{dt} = -\omega_M M.$$

4.8 The Model

The complete model is:

$$\begin{aligned} \frac{dD_I}{dt} &= A_1(C) - aD_I - a_T D_I \frac{T_R}{g_R + T_R} - \omega_I D_I \\ &\quad - b_T D_I \frac{I_{10}}{g_{10} + I_{10}} - k_{D_I} D_I (1 - e^{\delta_{D_I} M}) \end{aligned} \quad (4.11)$$

$$\frac{dD}{dt} = aD_I - \omega D - k_D D (1 - e^{\delta_D M}) \quad (4.12)$$

$$\begin{aligned} \frac{dD_T}{dt} &= a_T D_I \frac{T_R}{g_R + T_R} + b_T D_I \frac{I_{10}}{g_{10} + I_{10}} - \omega_T D_T \\ &\quad - k_{D_T} D_T (1 - e^{\delta_{D_T} M}) \end{aligned} \quad (4.13)$$

$$\frac{dT_N}{dt} = \alpha_N - \frac{\omega_N}{g_2 + I_2} T_N - k_N T_N (1 - e^{\delta_N M}) \quad (4.14)$$

$$\begin{aligned} \frac{dT_C}{dt} &= a_C T_N D + T_N A_2(C) - d_{D_T} T_C - a_{CP} T_C \frac{I_2}{g_2 + I_2} \\ &\quad + d_{CP} T_{CP} \frac{I_{10}}{g_{10} + I_{10}} - \omega_C T_C - k_C T_C (1 - e^{\delta_C M}) \end{aligned} \quad (4.15)$$

$$\begin{aligned} \frac{dT_{CP}}{dt} &= a_{CP} T_C \frac{I_2}{g_2 + I_2} - d_{CP} T_C \frac{I_{10}}{g_{10} + I_{10}} + \gamma T_{CP} - A_3(C) \\ &\quad - k_{CP} T_{CP} (1 - e^{\delta_{CP} M}) \end{aligned} \quad (4.16)$$

$$\frac{dT_R}{dt} = a_R D_T T_N + c T_R \frac{I_2}{g_2 + I_2} - \omega_R T_R - k_R T_R (1 - e^{\delta_R M}) \quad (4.17)$$

$$\frac{dI_2}{dt} = \alpha_2 T_N - \omega_2 I_2 + a_2 T_C \frac{I_2}{g_2 + I_2} \quad (4.18)$$

$$\frac{dI_{10}}{dt} = \alpha_{10} D_I + a_{10} T_R T_C - \omega_{10} I_{10} \quad (4.19)$$

$$\frac{dC}{dt} = fC(1 - hC) - D_C C - kC(1 - e^{\delta_C M}) \quad (4.20)$$

$$\frac{dM}{dt} = -\omega_M M \quad (4.21)$$

$$D_C = d \frac{(L/C)^l}{s + (L/C)^l} \quad (4.22)$$

Chapter 5

Mathematical Background

Typically when presented with a system of equations we may be tempted to try to solve them: find an analytic solution and then study the properties of that analytic solution. Unfortunately for large system of non-linear differential equations there may not be an analytical solution. Often the solution to such an equation is a function that is *defined* to be a solution to a particular differential equation, such as **Bessel Functions**. Instead of finding an exact solution there are several techniques that allow one to learn qualitative details about the system.

In general, we can analyze systems that are either linear or have few, ideally two or fewer, differential equations. The key, therefore, is to tweak the model so that it has one of these two properties. First, we will discuss **linear stability analysis** which can give a partial picture of the long term behavior of a linear or nonlinear system of any size. Second, we will discuss **phase plane analysis**, which can give qualitative information about the behavior of two-dimensional linear systems. Finally, we will discuss **seperation of time scales** which allows for the reduction of the dimensionality of a system.

5.1 Linear Stability Analysis

Linear stability analysis can be used to determine the stability of a system's equilibria. First we must find the equilibria by solving $\vec{f}(\vec{X}^*) = 0$. For the full system (see §4.8), this requires solving 11 nonlinear equations. It is unlikely that analytic solutions will exist for these equilibria and so some or all of the parameters will have to be fixed so that the solutions can be found numerically. As this is a biological system, we are only interested in

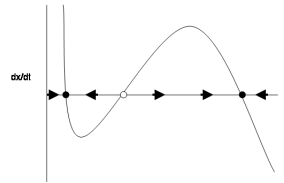


Figure 5.1: The derivative of the state variable plotted against its value. The black and white dots represent stable and unstable equilibrium respectively. The arrows show the direction of movement within state space.

equilibria that are real and positive.

Once the important equilibria have been found, we can compute their stability through linearization. At a given equilibrium point, \vec{X}^* , we approximate (1.1) as $\vec{X}' = A(\vec{X} - \vec{X}^*)$, where $A = J(\vec{X}^*)$ is the **Jacobian** of the system evaluated at $\vec{X} = \vec{X}^*$. The stability of each point can be found by computing the eigenvalues of the Jacobian. If all eigenvalues have a negative real part then the equilibrium point is stable, otherwise it is unstable.

5.2 Phase Plane Analysis

Phase plane analysis is a useful tool for two-dimensional systems. First, consider the *one*-dimensional canonical equation $X'(t) = f(X(t))$. Depending upon the function f , such an equation can be difficult to solve analytically. However, it is fairly simple to analyze the equation qualitatively. We can simply plot the function $f(X)$ and look for equilibria. An example is shown in Figure 5.1. Note that the sign of f determines which direction X moves along the axis. In this situation, the horizontal axis is referred to as **state space**. Position within state space is defined by the value of the state variable, in this case X . Using arrows to visualize dynamics, it is simple to determine the stability of each equilibrium without relying on phase plane analysis. There are very few possible behaviors in this, or indeed any, one-dimensional system. A solution could travel from one equilibrium to another, approach an equilibrium from infinity or approach infinity from an equilibrium.

The situation is not quite as simple if there are unknown parameters in

the equation. Changing a parameter could change the number and location of equilibrium points causing changes in the behavior of the system. Such changes are called **bifurcations**. Figure 5.2 illustrates the main types of bifurcations that occur in one-dimensional system. A **Transcritical Bifurcation** occurs when two equilibria exchange stability, a **Saddle-Node Bifurcation** occurs when one stable and one unstable equilibrium both appear simultaneously, and a **Pitchfork Bifurcation** occurs when one equilibrium splits into three.

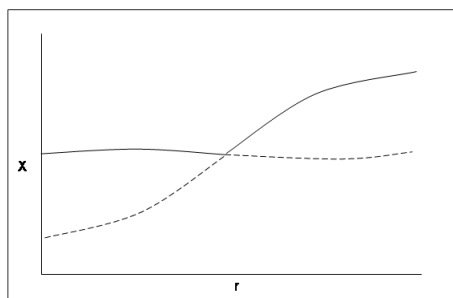
We can apply similar qualitative reasoning in two-dimensional systems. Suppose we have the following system:

$$\frac{dX_1}{dt} = f_1(X_1, X_2) \quad (5.1)$$

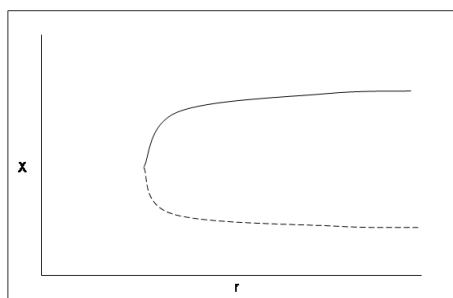
$$\frac{dX_2}{dt} = f_2(X_1, X_2). \quad (5.2)$$

First, we set (5.1) equal to zero and find a relation between X_1 and X_2 . We plot the points that satisfy this relation as in Figure 5.3. This resulting curve is the X_1 -**nullcline**. We find the X_2 -nullcline analogously. The nullclines divide the state space into regions. In each region, we can readily determine the sign but not the magnitude of the vector field. As in the one-dimensional case, we can infer, often, stability of equilibria without the need for linear stability analysis. There are more possible behaviors in two-dimensional systems. As before, trajectories may travel between points, **heteroclinic orbits**, move from an equilibrium to infinity or to infinity from an equilibrium. In addition, trajectories may form a closed loop or start end finish at the same equilibrium (**homoclinic orbit**).

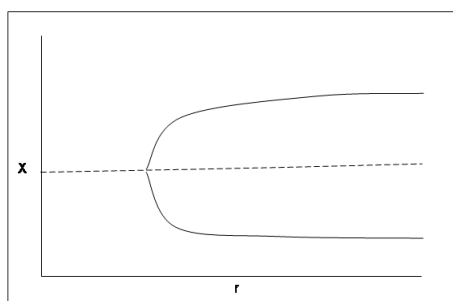
Another feature of two-dimensional systems that one-dimensional ones lack are **saddle points**. These are points whose Jacobian has some eigenvalues with positive real part and some with negative. In a two dimensional system, it is necessarily the case that there will be exactly one positive and one negative eigenvalue associated with a saddle point. Saddle points are unstable, in that, nearby trajectories tend not to stay nearby. There are regions of state space which move toward a saddle point. In fact, as depicted in Figure 5.3 there is one trajectory, often two, that do asymptotically approach the saddle point. These trajectories are called **stable manifolds** and they have a counterpart **unstable manifolds** which approach the saddle point going backwards in time. The importance of stable manifolds is their role as **separatrices**, meaning that they divide state space into regions with fundamentally different behavior. As different trajectories cannot cross each other, each one is trapped on one side of the stable manifold.



(a) Transcritical Bifurcation



(b) Saddle Node Bifurcation



(c) Pitchfork Bifurcation

Figure 5.2: The bifurcations that can occur in one dimensional systems. Each figure shows the equilibria plotted against a generic parameter, r . Solid and dashed lines represent stable and unstable equilibria respectively.

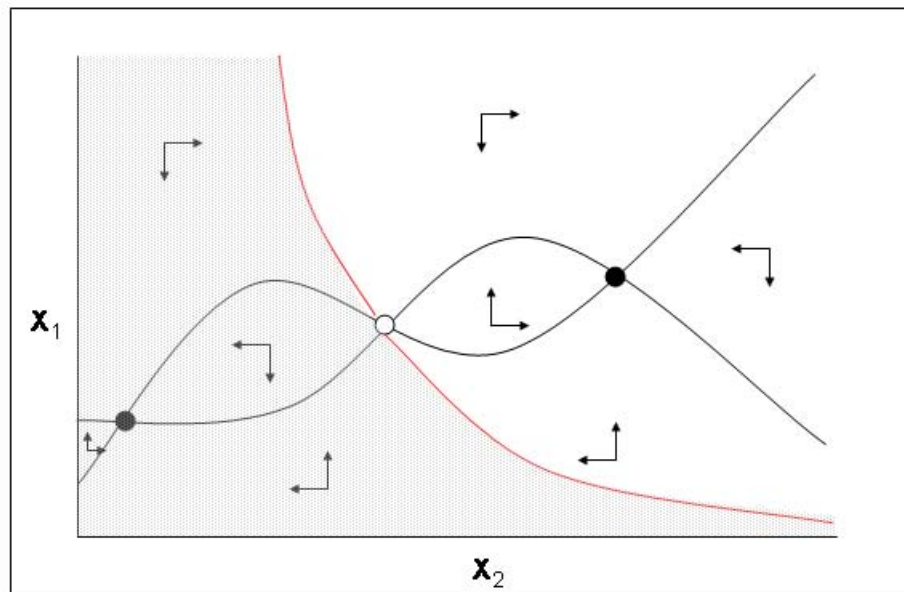


Figure 5.3: A generic phase plane of a two dimensional ODE system. The black curves represent the nullclines of the state variables and the black and white circles show node and saddle points respectively. The arrows show the sign of the derivative in each region and the red curve is the stable manifold of the saddle point. It is also marks the boundary of the basin of attraction of the left equilibrium point (shaded in gray). The remainder of the plot is in the basin of attraction of the right equilibrium point.

Position with respect to the manifold therefore might determine which of several stable equilibria the trajectory approach asymptotically or whether they can approach an equilibrium at all. For this reason, a manifold might define the edge of a **basin of attraction**, the set of all points in state space, whose trajectories lead asymptotically towards a particular point.

5.3 Separation of Time Scales

Systems with greater than two differential equations are tough to analyze, not only because they have more equations, but also because there are a greater variety of ways in which they can behave. Sometimes, however a higher dimensional system may behave approximately like a system with two or fewer equations. The synthesis and decay of cytokines, turnover of T-cells, and turnover of dendritic cells all take place at different rates. The rates are so different, in fact, that we would place them in separate time scales. To understand how this simplifies the system, we can imagine that we wish to model the distribution of mass in a bookcase infested with termites. Let's suppose that at some point the bookshelf collapses suddenly. As it collapses it does not make any sense to model the effect of the termites eating, as the change is too slow to affect the dynamics of the collapse significantly.

For a more mathematical example, let's suppose that we have a system of three equations,

$$\begin{aligned}\frac{dX_1}{dt} &= f_1(X_1, X_2, X_3) \\ \frac{dX_2}{dt} &= \epsilon f_2(X_1, X_2, X_3) \\ \frac{dX_3}{dt} &= \epsilon^2 f_3(X_1, X_2, X_3).\end{aligned}$$

For small $\epsilon > 0$, only the derivative of X_1 is non-negligible, in which case we can approximate the other variables as constant. Therefore we can reduce the system to

$$\frac{dX_1}{dt} = f_1(X_1, X_2(t_0), X_3(t_0)) = f(X_1).$$

Assuming this is a biological system, we assume that state variables will not approach infinity. In the one dimensional case, we know that X_1 must instead approach an equilibrium, which can be easily determined from the

roots of f , the initial value $X_i = X_1(t_0)$ and the sign of $f(X_i)$. If $f(X_i)$ is positive then we know that X_1 will approach the smallest root of f greater than X_i . If negative, X_1 will approach the largest root of f less than X_i .

Now, still assuming $\epsilon > 0$ is small, we consider a new time scale $t_1 = \epsilon t$. Note that X_1 will now always be at or near its equilibrium. The new time derivative $\frac{d}{dt_1} = \frac{1}{\epsilon} \frac{d}{dt}$, so the system can be expressed as

$$\begin{aligned} \frac{dX_2}{dt_1} &= f_2(X_1, X_2, X_3) \\ \frac{dX_3}{dt_1} &= \epsilon f_3(X_1, X_2, X_3). \end{aligned}$$

As X_3 does not change significantly in this time scale, the dynamics are again approximately one dimensional ($X_2' = f(X_2)$) and we can perform the same analysis. Splitting up the behavior in this manner allows us to gain important insights on the dynamics that would otherwise require heavy computation. In particular, we can find the **basin of attraction** of each equilibrium, or the set of all initial conditions which asymptotically approach the given equilibrium point.

Chapter 6

Infection-Free Dynamics

6.1 Derivation of the Reduced Model

In the absence of infection, the activation functions $A_i(C)$ must be set to zero. We can then rewrite (4.1)-(4.3) as:

$$\frac{dD_I}{dt} = -\left(a + a_T \frac{T_R}{g_R + T_R} + \omega_I + b_T \frac{I_{10}}{g_{10} + I_{10}}\right) D_I \quad (6.1)$$

$$\frac{dD}{dt} = aD_I - \omega D \quad (6.2)$$

$$\frac{dD_T}{dt} = a_T D_I \frac{T_R}{g_R + T_R} + b_T D_I \frac{I_{10}}{g_{10} + I_{10}} - \omega_T D_T. \quad (6.3)$$

Summing all three equations together yields

$$\frac{dD_{Tot}}{dt} = -\omega_I D_I - \omega D - \omega_T D_T, \quad (6.4)$$

which indicates that all dendritic cell populations decay toward zero over time. Therefore, when there is no infection we need only consider the re-

duced model:

$$\frac{dT_N}{dt} = \alpha_N - \frac{\omega_N}{g_2 + I_2} T_N \quad (6.5)$$

$$\frac{dT_C}{dt} = -a_{CP} T_C \frac{I_2}{g_2 + I_2} + d_{CP} T_{CP} \frac{I_{10}}{g_{10} + I_{10}} - \omega_C T_C \quad (6.6)$$

$$\frac{dT_{CP}}{dt} = a_{CP} T_C \frac{I_2}{g_2 + I_2} - d_{CP} T_{CP} \frac{I_{10}}{g_{10} + I_{10}} + \gamma T_{CP} \quad (6.7)$$

$$\frac{dT_R}{dt} = c T_R \frac{I_2}{g_2 + I_2} - \omega_R T_R \quad (6.8)$$

$$\frac{dI_2}{dt} = \alpha_2 T_N - \omega_2 I_2 + T_C \frac{I_2}{g_2 + I_2} \quad (6.9)$$

$$\frac{dI_{10}}{dt} = a_{10} T_R T_C - \omega_{10} I_{10}. \quad (6.10)$$

After non-dimensionalization, the system becomes:

$$\frac{dT_N}{dt} = 1 - \frac{\omega_N}{1 + I_2} T_N \quad (6.11)$$

$$\frac{dT_C}{dt} = -a_{CP} \left(T_C \frac{I_2}{1 + I_2} + d_{CP} T_{CP} \frac{I_{10}}{1 + I_{10}} \right) - \omega_C T_C \quad (6.12)$$

$$\frac{dT_{CP}}{dt} = d_{CP} \left(T_C \frac{I_2}{1 + I_2} - T_{CP} \frac{I_{10}}{1 + I_{10}} \right) + \gamma T_{CP} \quad (6.13)$$

$$\frac{dT_R}{dt} = c T_R \frac{I_2}{1 + I_2} - \omega_R T_R \quad (6.14)$$

$$\frac{dI_2}{dt} = \alpha_2 T_N - \omega_2 I_2 + T_C \frac{I_2}{1 + I_2} \quad (6.15)$$

$$\frac{dI_{10}}{dt} = T_R T_C - \omega_{10} I_{10}. \quad (6.16)$$

6.2 Analysis

6.2.1 Equilibrium Points

To analyze the reduced system, first we set (6.11)-(6.16) to zero and solve them as a system to find the equilibrium points. As this is a biological model, we are interested only in positive equilibria. The system has either zero, one or two equilibria depending upon parameters. The first point,

which we shall call \vec{X}_1 , is given by:

$$T_R = T_C = T_{CP} = I_{10} = 0 \quad (6.17)$$

$$T_N = \frac{\omega_2}{\omega_2\omega_N - \alpha_2} \quad (6.18)$$

$$I_2 = \frac{\alpha_2}{\omega_2\omega_N - \alpha_2}. \quad (6.19)$$

It is positive if and only if

$$\frac{\alpha_2}{\omega_2\omega_N} = R_1 < 1. \quad (6.20)$$

Naive T-cells produce IL-2 which in turn lowers the death rate of the naive T-cells. If IL-2 is produced at too high of a rate, so that $R_1 > 1$, then there will be unending positive feedback and both populations will rise indefinitely regardless of antigen stimulation. Therefore we constrain $R_1 < 1$. The eigenvalues of \vec{X}_1 are

$$\lambda_1 = \gamma \quad (6.21)$$

$$\lambda_2 = -\omega_{10} \quad (6.22)$$

$$\lambda_3 = -\omega_C - \frac{a_{CP}\alpha_2}{\omega_2\omega_N} \quad (6.23)$$

$$\lambda_4 = -\omega_R + \frac{c\alpha_2}{\omega_2\omega_N} \quad (6.24)$$

$$\lambda_{5,6} = \frac{-\omega_N\omega_2^2 - \omega_N^2\omega_2 + \alpha_2\omega_N}{2\omega_2\omega_N} \quad (6.25)$$

$$\pm \frac{\sqrt{(\omega_N\omega_2^2 + \omega_N^2\omega_2 - \alpha_2\omega_N)^2 - G}}{2\omega_2\omega_N} \quad (6.26)$$

$$G = 4\omega_2\omega_N (\alpha_2^2 - 2\alpha_2\omega_2\omega_N + \omega_2^2\omega_N^2). \quad (6.27)$$

This equilibrium point is always a saddle point as λ_1 is always positive whereas λ_2 and λ_3 are always negative. λ_4 is positive if and only if $R_1R_2 > 1$. Finally, given that $R_1 < 1$, the real parts of λ_5 and λ_6 are always negative.

The second point, which we shall call \vec{X}_2 , is given by:

$$T_R = \frac{\gamma^2 \omega_{10} \omega_N (c - \omega_R) \omega_R (c \omega_C + a_{CP} \omega_R)}{c a_{10} \omega_C (c (\gamma - d_{CP}) \omega_C + \gamma a_{CP} \omega_R) (c \alpha_2 - \omega_2 \omega_N \omega_R)} \quad (6.28)$$

$$T_N = \frac{c}{\omega_N (c - \omega_R)} \quad (6.29)$$

$$T_C = \frac{c (\omega_2 \omega_N \omega_R - c \alpha_2)}{a_2 \omega_N (c - \omega_R) \omega_R} \quad (6.30)$$

$$T_{CP} = \frac{c \omega_C (\omega_2 \omega_N \omega_R - c \alpha_2)}{\gamma \omega_N (c - \omega_R) \omega_R} \quad (6.31)$$

$$I_{10} = -\frac{\gamma (c \omega_C + a_{CP} \omega_R)}{c (\gamma - d_{CP}) \omega_C + \gamma a_{CP} \omega_R} \quad (6.32)$$

$$I_2 = \frac{\omega_R}{c - \omega_R}. \quad (6.33)$$

This point is positive if and only if all of the following are true:

$$R_1 < 1 \quad (6.34)$$

$$\frac{c}{\omega_R} = R_2 > 1 \quad (6.35)$$

$$R_1 R_2 < 1 \quad (6.36)$$

$$d_{CP} > \gamma \left(1 + \frac{a_{CP}}{\omega_R R_2}\right). \quad (6.37)$$

Although it is difficult to find the eigenvalues of this point, as they are the roots of a 6th degree polynomial, we may still compute the determinant of the Jacobian:

$$\|J(\vec{X}_2)\| = \gamma \omega_{10} (c - \omega_R)^2 (c \omega_C + a_{CP} \omega_R) \quad (6.38)$$

$$\times \frac{(c (\gamma - d_{CP}) \omega_C + \gamma a_{CP} \omega_R) (c \alpha_2 - \omega_2 \omega_N \omega_R)}{c^4 d_{CP} \omega_C}. \quad (6.39)$$

The determinant is positive whenever \vec{X}_2 is positive. If the determinant had been negative then at least one eigenvalue would have been positive. As it stands, however, the stability of \vec{X}_2 is inconclusive.

6.2.2 Transient Behavior

Linear stability analysis failed to reveal an asymptotically stable equilibrium point. We must ensure that solution trajectories remain bounded and not grow to infinity. Unbounded solutions cannot be valid in a biological

setting. To determine whether the system is bounded we rewrite the reduced model assuming that all state variables have grown arbitrarily large. Specifically we say that:

$$cc \frac{I_2}{I_2 + 1} = 1 \quad \text{as } I_2 \gg 1 \quad (6.40)$$

$$\frac{1}{I_2 + 1} = 1/I_2 \quad \text{as } I_2 \gg 1 \quad (6.41)$$

$$\frac{I_{10}}{I_{10} + 1} = 1 \quad \text{as } I_{10} \gg 1 \quad (6.42)$$

The rewritten system is:

$$\frac{dT_N}{dt} = 1 - \frac{\omega_N}{I_2} T_N \quad (6.43)$$

$$\frac{dT_C}{dt} = -a_{CP} T_C + d_{CP} T_{CP} - \omega_C T_C \quad (6.44)$$

$$\frac{dT_{CP}}{dt} = a_{CP} T_C - d_{CP} T_C + \gamma T_{CP} \quad (6.45)$$

$$\frac{dT_R}{dt} = c T_R - \omega_R T_R \quad (6.46)$$

$$\frac{dI_2}{dt} = \alpha_2 T_N - \omega_2 I_2 + a_2 T_C \quad (6.47)$$

$$\frac{dI_{10}}{dt} = T_R T_C - \omega_{10} I_{10}. \quad (6.48)$$

First we can see that (6.44) and (6.45) form a linear system, decoupled from the other equations. To ensure that this subsystem is bounded, we must show that the origin is an attractor. As it is a linear system we can write it in the form

$$x'(t) = Ax(t) \quad (6.49)$$

where

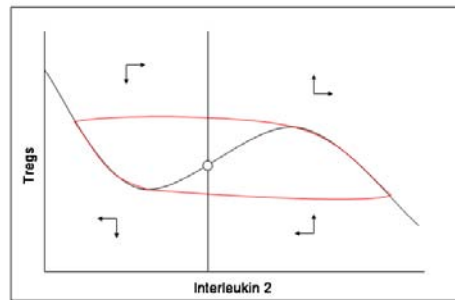
$$A = \begin{pmatrix} -(a_{CP} + \omega_C) & d_{CP} \\ a_{CP} & \gamma - d_{CP} \end{pmatrix}.$$

In order for this linear system to be stable, both eigenvalues of A must have negative real part which is equivalent to the determinant being positive and the trace being negative. Both of these conditions are met if and only if $d_{CP} < \gamma(1 + a_{CP}/\omega_C)$.

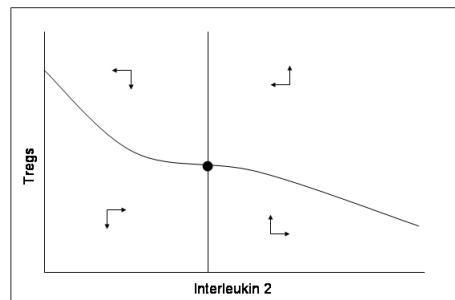
6.3 Limit Cycle

If the system is bounded and there are no stable equilibrium points, then there exists the possibility of a **limit cycle**. This is a trajectory that continually revisits the same points repeatedly and which nearby trajectories approach asymptotically. In a two dimensional system we can prove the existence of a limit cycle by demonstrating that there is a **trapping region** in state space. This a region that trajectories cannot leave once they are inside it. By the **Poincaré Bendixson** we know these trajectories will either move towards a stable equilibrium point or enter a limit cycle. If we can demonstrate that there exist no stable points within the trapping region, then we know that there is a limit cycle. We already know that the system is bounded so we can find such a region as long as \vec{X}_2 is stable.

The existence of this region does not imply that there exists a limit cycle as the system has more than two dimension. If we build a little intuition about the system however, we will see that the system behaves as though it were two dimensional. Consider (6.14). When the right-hand side is equal to zero, we see that $\frac{l_2}{1+l_2} > \frac{c}{\omega_R - c}$. So when IL-2 is present in high levels T_R grows otherwise it shrinks. Given that regulatory T-cells are on a much slower time scale, we may assume that IL-2 is in equilibrium. Figure 6.1 shows the two types of behavior that can arise from this. Note that the limit cycle arises when the relationship between Tregs and IL-2 is non-monotonic. If it is monotonic then cytotoxic T-cells will never rise above the a certain point. The system appears to act like a switch, if the cytotoxic T-cells are at a high enough level, then regulatory T-cells are gradually activated to reduce them after a delay. When there is no limit cycle, the system hovers perpetually around the switch level. Due to these biological considerations, for the remaining analysis we shall use parameters that do yield a limit cycle.



(a) Limit Cycle



(b) No Limit Cycle

Figure 6.1: The two possible behaviors of the reduced model. The black lines represent nullclines and the black and white dots represent stable and unstable points. In the top picture, the red curve represents the limit cycle.

Chapter 7

Adapting the Model

Due to the large number of unknown parameters and the large number of equations, the full model remains difficult to analyze. In this chapter, we shall attempt to make simplifying changes to the model without stripping it of its predictive power.

7.1 Removal of Naive T-Cell Population

The only way in which the Naive T-cell population can differ from a source time is if it enters a positive feedback loop with the level of IL-2. In §6.2, we constrained the parameters to preclude that from happening for otherwise both populations would rise unchecked. Infinite exponential growth of these populations would be unacceptable in a biological system. Therefore, the population should either assumed to be constant or other terms should be added to the equation to curtail the growth. We assume that the population is constant and remove it from the equations except as a source term.

7.2 Separating the Cytokine Time Scale

Given the rapid decay rate of IL-2 and IL-10 within the body we shall assume as in §6.3 that the levels of these chemicals is entirely dependent upon the levels of T_C and T_R . This yields the following expressions for IL-2 and

IL-10:

$$\frac{I_2}{1 + I_2} = \frac{T_C - \alpha_2 - \omega_2 + \sqrt{(-T_C + \alpha_2 + \omega_2)^2 + 4T_C\alpha_2}}{2T_C} \quad (7.1)$$

$$I_{10} = \frac{T_R T_{CP}}{\omega_{10} + T_R T_{CP}}. \quad (7.2)$$

The expression for IL-2 is extremely complicated compared to the actual behavior that it describes. It can be replaced by $\frac{T_C^2}{k_2 + T_C^2}$ where $k_2 = 1000$. Although it is not exactly the same, the original curve only represents a model based upon an arbitrary non-linearity. Therefore, there is no reason to believe that this curve is any worse than the original, yet it is much simpler.

7.3 Removal of Dendritic Cell Populations

The focus of this model is on the effect of IL-2 therapy. Seeing as do not have estimates for many of the parameters in the dendritic cell populations, it would seem prudent to remove them. However, we may still create a model that reflects the following assumptions that were in the original model.

- When a foreign antigen enters the body, dendritic cells stimulate the production of antigen specific T-cells.
- When the antigen is present at high levels, tolerogenic dendritic cells prevent antigen specific T-cells from proliferating.
- Regulatory T-cells and tolerogenic T-cells have positive feedback meaning that when there are more Tregs, there is a higher level of tolerance coming from dendritic cells

To accomplish all of this, let us assume that the total number of antigen specific dendritic cells within the body is a function of the size of the tumor. Specifically, we shall use the following term from [5]:

$$D_{\text{Total}} = \frac{C}{k_C + C}.$$

In its original context this term modelled the activation rate of the cytotoxic T-cell population via antigen stimulation. Now we shall assume that

some of these dendritic cells are immunogenic and some are tolerogenic. The fraction that are immunogenic rises with increased antigen stimulation and increased levels of regulatory T-cells. We can express this fraction as

$$p = \frac{C^2}{1 + C^2} \frac{T_R}{k_R + T_R}.$$

Therefore, the numbers of tolerogenic and immunogenic dendritic cells are pD_{Total} and $(1 - p)D_{\text{Total}}$ respectively. Note that initially the number of immunogenic dendritic cells will increase, but eventually the total number of dendritic cells will plateau and the proportion that are immunogenic will decrease to close to zero. This means that the strongest immune response will be against an antigen present in intermediate amounts as opposed to something ubiquitous or present in insignificant amounts.

Given that we now assume a constant level of naive T-cells, the source term for cytotoxic T-cells is only dependent upon levels of immunogenic dendritic cells. We assume that tolerogenic dendritic cells kill contribute to lowering the net proliferation rate of cytotoxic T-cells. They do this both through direct deletion and also through stimulation of Regulatory T-cells. Given all of these changes, the new system of equations is as follows.

$$\begin{aligned} \frac{dT_C}{dt} &= -T_C + g_I \frac{C}{C + k_C} \left(1 - \frac{C^2}{(C^2 + 1)} \frac{T_R}{(k_R + T_R)} \right) \\ &\quad - a_{CP} \left(\frac{T_C^3}{T_C^2 + k_2} - \frac{T_{CP}^2 T_R}{\omega_{10} + T_{CP} T_R} \right) \end{aligned} \quad (7.3)$$

$$\begin{aligned} \frac{dT_{CP}}{dt} &= T_{CP} \left(\gamma - g_T \frac{C^2}{(C^2 + 1)} \frac{C}{(C + k_C)} \frac{T_R}{(k_R + T_R)} \right) \\ &\quad + d_{CP} \left(\frac{T_C^3}{T_C^2 + k_2} - \frac{T_{CP}^2 T_R}{\omega_{10} + T_{CP} T_R} \right) \end{aligned} \quad (7.4)$$

$$\frac{dT_R}{dt} = c T_R \frac{T_C^2}{T_C^2 + k_2} - \omega_R T_R \quad (7.5)$$

$$\frac{dC}{dt} = fC(1 - hC) - d \frac{(T_C + T_{CP}/C)^l}{s + (T_C + T_{CP}/C)^l} C \quad (7.6)$$

Chapter 8

Analyzing the new Model

In the previous chapter, we derived the following system of four equations in an attempt to capture the behavior of the more complete model:

$$\begin{aligned} \frac{dT_C}{dt} &= -T_C + g_I \frac{C}{C + k_C} \left(1 - \frac{C^2}{(C^2 + 1)} \frac{T_R}{(k_R + T_R)} \right) \\ &\quad - a_{CP} \left(\frac{T_C^3}{T_C^2 + k_2} - \frac{T_{CP}^2 T_R}{\omega_{10} + T_{CP} T_R} \right) \end{aligned} \quad (8.1)$$

$$\begin{aligned} \frac{dT_{CP}}{dt} &= T_{CP} \left(\gamma - g_T \frac{C^2}{(C^2 + 1)} \frac{C}{(C + k_C)} \frac{T_R}{(k_R + T_R)} \right) \\ &\quad + d_{CP} \left(\frac{T_C^3}{T_C^2 + k_2} - \frac{T_{CP}^2 T_R}{\omega_{10} + T_{CP} T_R} \right) \end{aligned} \quad (8.2)$$

$$\frac{dT_R}{dt} = c T_R \frac{T_C^2}{T_C^2 + k_2} - \omega_R T_R \quad (8.3)$$

$$\frac{dT_C}{dt} = fC(1 - hC) - d \frac{(T_C + T_{CP}/C)^l}{s + (T_C + T_{CP}/C)^l} C. \quad (8.4)$$

To analyze this model, we will consider two separate time scales as in §5.3. First, we observe that, numerically, the values of (8.1) and (8.2) are the much greater than the values of (8.3) and (8.4). Using this knowledge, we can approximate that (8.3) and (8.4) are equal to zero when analyzing the behavior of (8.1) and (8.2). Figure 8.1 shows qualitatively the possible shapes of the nullclines of both (8.1) and (8.2). We see that there are either one or three equilibrium points, except right at the bifurcation points where there are two. We also see that both the high and low equilibria will be stable whereas the the intermediate equilibrium is unstable. It is also important

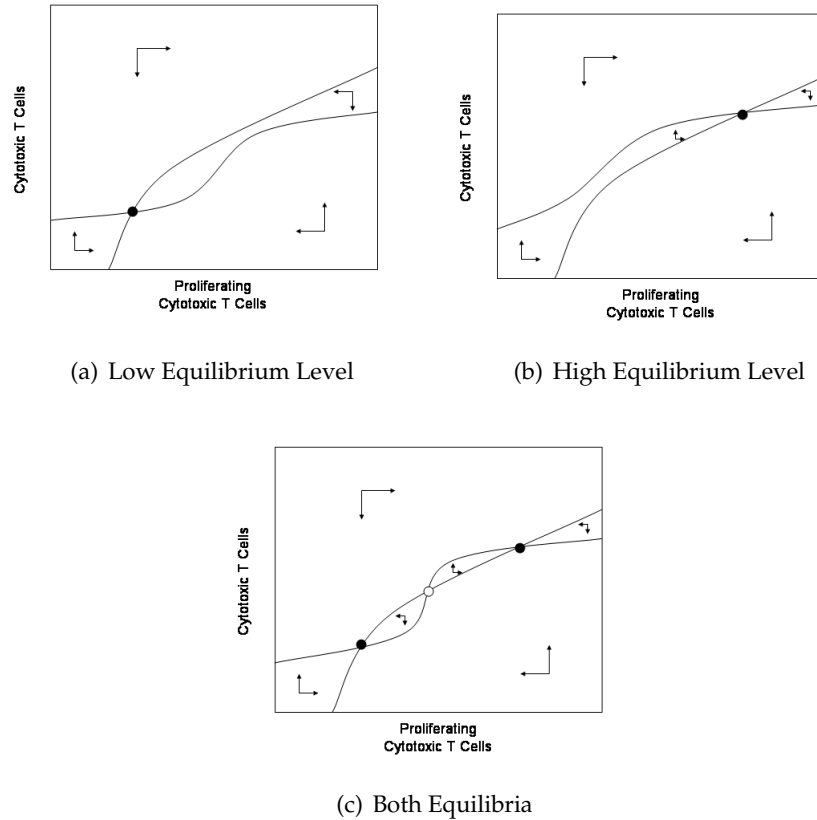


Figure 8.1: Qualitative phase portraits for the fast time scale. Depending upon the values of T_R and C , the system has either one or three equilibria.

to note that the scales on these plots are logarithmic, so the values of the equilibria differ by orders of magnitude. Two distinct saddle node bifurcations occur between plots 1 and 2 and between plots 2 and 3 on Figure 8.1. These bifurcations take place as we change C and T_R which act as parameters in this planar system.

Suppose we have a situation where there are 3 equilibria and the system is currently at rest at the lower equilibrium. We may then tune the parameters C and T_R so that the lower equilibrium no longer exists. This will force the system to move to the higher equilibrium. Changing C and T_R back to their initial values does not make the system return to its initial equilibrium point. This irreversibility is known as **hysteresis**. In the context

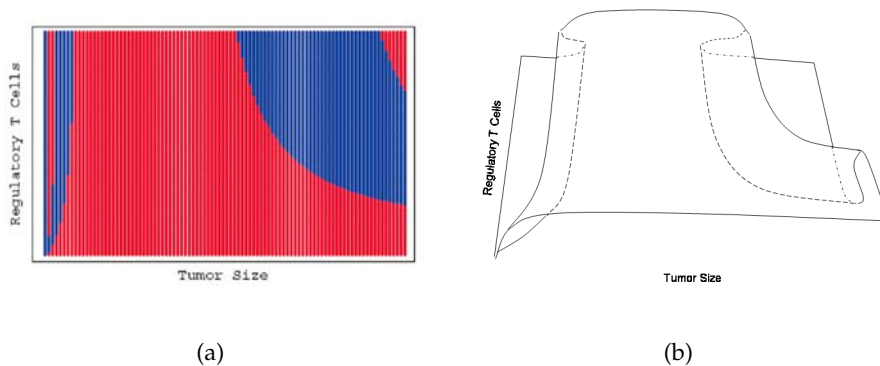


Figure 8.2: The slow time scale takes place on a folded surface. The left panel shows the areas where there are one (red) and three (blue) equilibria. The right panel shows a qualitative 3D representation of the surface, where the third dimension is total cytotoxic T-cells.

of this model, that means that sudden, extreme and irreversible changes in the levels of cytotoxic T-cells should be expected.

Because of hysteresis, the two dimensional system of (8.3)-(8.4) cannot simply be analyzed using phase plane analysis. A crucial assumption in phase plane analysis is that the trajectory is entirely dependent upon the two-dimensional location in state space. Given that hysteresis occurs at some points, the trajectory of the system will depend not only upon the values of the state variables, in this case C and T_R , but also the path taken to get to that point in state space. Despite this, we may still visualize the dynamics in a similar manner, recognizing that trajectory is not moving through a plane but over a more complicated surface. Figure 8.2 shows the regions of state space where (8.1)-(8.2) have three solutions in blue, regions with one solution are shown in red. The picture translates into a surface qualitatively similar to that shown in the right panel of Figure 8.2. The third dimension is an approximate sum of proliferating and non-proliferating cytotoxic T-cells. Representing both separately would not only require a four dimensional picture but also confer little additional information as the equilibrium levels of T_C and T_{CP} are almost directly proportional to one another. The “lips” in this case represent the point where the bifurcation occurs and there is a sudden change in T-cell levels. Such a sudden change is referred to as a **catastrophe**.

Although it is possible to draw the nullclines on this surface, it is made

more challenging than normal because it is multivalued in some places. In Figure 8.3 we see the different possibilities for the dynamics of the tumor. The dark blue dots represent areas where there is only one stable surface and the tumor is shrinking. The red dots, indicate that there is only one stable surface and the tumor is growing. The green dots indicate that there two stable surfaces and the tumor is growing on both of them. The yellow dots indicate that on one surface the tumor is growing and on the other the tumor is shrinking. Finally, the light blue dots indicate that there are two stable surfaces and the tumor is shrinking on both. Given current parameter values it is almost always the case that regulatory T-cells grow on the lower surface and rise on the upper surface. Therefore we may refer to Figure 8.2 to assess where the T_R -nullclines lie.

Note that many of the parameter values are only estimated and so the precise position of each region is not relevant. We can see however that, regulatory T-cells must be at a low-level in order for a large tumor to shrink down. The trajectory must be able to pass below the red region. We can also see that a large tumor may go through small oscillations. In the yellow region, it shrinks on the upper surface and the regulatory T-cells grow. When it reaches the boundary of this region, the trajectory starts traveling in the opposite direction until it hits the other side. Therefore, we can imagine that a large tumor's trajectory is bouncing back and forth within the yellow region.

It's important to note that the administration of IL-2 therapy should move a trajectory almost instantaneously from the lower surface to the upper one. We can see that a one time dose of IL-2 will not have much effect, as the trajectory will remain trapped in the yellow region. If the red region moves up and exposes the left side of the yellow region. Then it may be possible for IL-2 to allow the trajectory to escape, as, once it is inside the blue region, the tumor continues to shrink. Chemotherapy or different parameter choices, would be required to move the red region upward.

Under certain parameters, it is possible that very interesting dynamics may occur when the tumor is small. Figure 8.4 shows the a qualitative diagram of behavior in such a situation. The thick red curves indicate where there are catastrophes. Between the two, there are two stable surfaces. In the region with two stable surfaces, curves that belong on the lower surface are dashed whereas curves that belong on the upper surface are solid. The black curves represent the C-nullclines and the arrows qualitatively represent the direction a trajectory must take through state space. The T_R -nullclines overlap with the red lines, but it is important to remember that T_R increases on the upper surface and decreases on the lower surface. Fi-

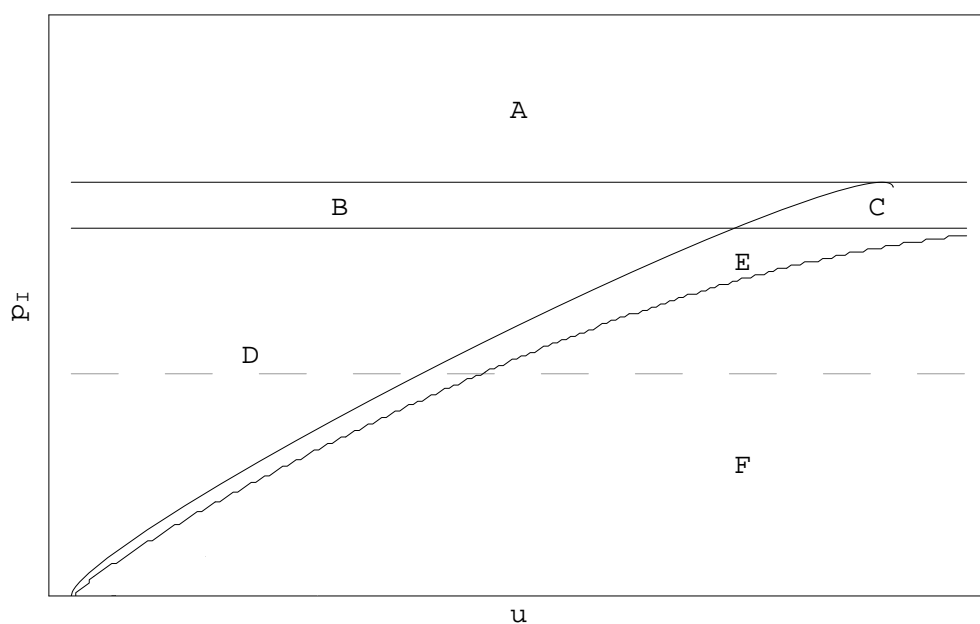


Figure 8.3: The red region indicates that there is only one stable surface and the tumor is growing. The green region indicates that there are two stable surfaces and the tumor is growing on both of them. The yellow region indicates that on one surface the tumor is growing and on the other the tumor is shrinking. Finally, the light blue region indicates that there are two stable surfaces and the tumor is shrinking on both.

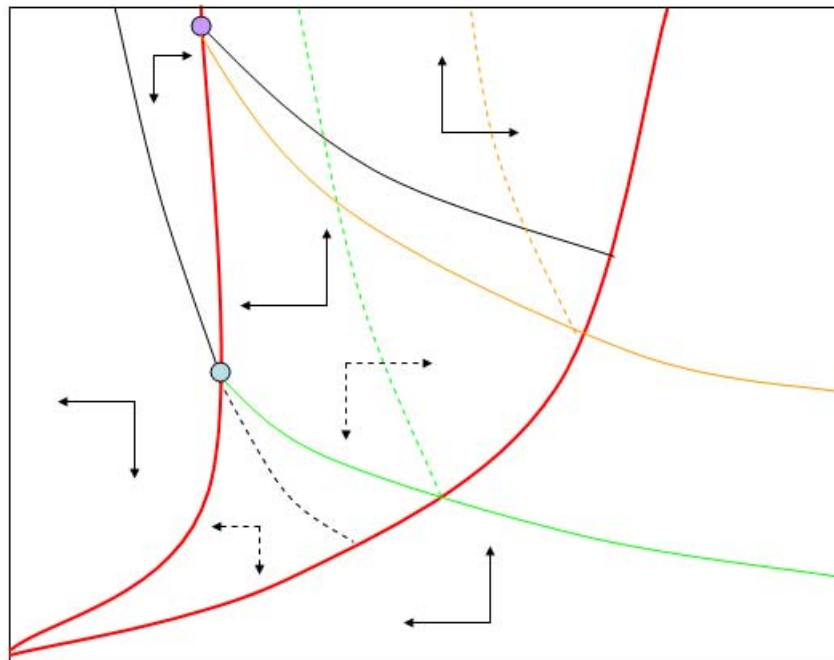


Figure 8.4: Between the thick redlines the surface is folded onto itself. The green and orange lines represent the stable manifolds of the blue and purple points respectively. Dotted lines are on the lower surface.

nally, the green and orange curves represent the stable manifolds of the blue and purple points respectively. These points are not true equilibrium points, however there is a sign change of the derivatives of both state variables at these points. It is not an equilibrium because the sign change does not occur on any of surfaces but rather in between them and cytotoxic T-cells are only in equilibrium exactly on the surfaces. The blue point is significant as its manifold defines the edge of the basin of attraction for the zero tumor equilibrium point. Below the solid green curve any trajectory on the upper surface is eventually forced towards the origin. On the lower surface, any trajectory below the dashed green curve is forced to the origin. Curves on either surface can bounce back and forth between the two red curves meaning that true edge of the basin of attraction is not readily defined. Points, above the orange curve on their respective surface will not approach the zero tumor equilibrium but rather escape to a large tumor equilibrium. In summary, trajectories below the green curves on their surface will shrink quickly. Points between the green and orange curves will shrink eventually. Points above the orange curve will grow to a full size tumor.

From this we can extract a key observation. Consider the small region above the solid orange curve and below the dashed green curve. On the lower surface, the point is below the green curve so all trajectories starting in this region go to the origin quickly. On the upper surface all trajectories will grow into a full size tumor. In fact, it is the case for any point in the region bounded by the dashed and solid orange curves that trajectories on the lower surface will shrink and trajectories on the upper surface will grow to a full size. This means that if IL-2 therapy is administered while the system is in this state, the treatment will kick the system out of the basin of attraction of the zero tumor equilibrium point. Once this has been done, it is impossible to reverse with future treatments. This would be an extremely unfortunate situation as it would nullify the effects of a long treatment schedule unless chemotherapy were given promptly to force the tumor back down again.

Chapter 9

Conclusion

9.1 Lessons From the Model

Treatment with IL-2 has mixed results and it is easy to see why when we consider all the different ways that it interacts with the immune system. Here we created and analyzed a model of an antigen specific immune response to cancer. The hope was to hopefully provide some qualitative information as to how to control this system with treatment. The important observation is that appropriateness of IL-2 treatment depends upon the size of the tumor. For an extremely large tumor, which in this case was one at its logistic carrying capacity, it can be useful to give IL-2 treatment initially. It may be necessary to also give chemotherapy to also see a significant effect.

However, in smaller tumors, around one tenth of the size, it could very well be detrimental to administer IL-2. When the tumor is at this size, the immune system is continuously mounting short lived responses that eventually become large enough to destroy the tumor entirely without help from chemotherapy drugs. The effect of giving IL-2 therapy in this situation is similar to pushing a child on a swing at the wrong time. Instead of adding to the immune response, the immunotherapy drug actually greatly reduces it. This brief interruption of the immune system allows the tumor to overwhelm it and grow back to a large size.

When a patient is not making any progress under a particular treatment schedule, it may be possible that this or a similar process is allowing the cancer to return each time. Patients that are not responding well could have their T-cell counts measured directly before and after administration of IL-2 to determine whether this is happening. After administration there should be an increase in regulatory T-cells and decrease in cytotoxic T-cells

compared to before. As the immune system is cycling it may be necessary to take several measurements over a period of several weeks to determine how the administration of the drug affected the cycle. If there is a decrease, then it may be worth repeating the cycle but ceasing IL-2 administration at an earlier point.

Unfortunately, it is difficult to observe exactly what is occurring in the body at any point in time. In this paper, we assume that the body is a well-mixed system, that the concentration of each quantity is distributed uniformly. The truth is that a blood sample may not accurately reflect the average behavior of the system. Similarly, the change in the system may be so subtle that it cannot be clinically detected. Therefore, the recommendation of using IL-2 therapy less later on in treatment should be kept in mind if all else fails. It would not be reasonable to plan to stop using IL-2 treatment at the moment when a tumor is no longer clinically detectable. In truth, much more information needs to be gathered on this phenomenon before it can be manipulated in a clinical setting.

9.2 Future Work

To start with, there is more analysis that can be performed on this model. The parameters need to be fit to data instead of assigned ad-hoc, as many are now. Assuming that we know all parameters with reasonable certainty, we can use a technique known as **optimal control**. This is a method to systematically find a solution that simultaneously satisfies all of these conditions. Previous models of cancer treatment have been subjected to optimal control ([5],[10]).

First we must define an **objective functional**, which takes one or more functions as an argument and returns a number. In this case we might use an objective functional of the following form:

$$J(u_1, u_2) = \int_{t=0}^{t_f} \eta_1 u_1(t) + \eta_2 u_2(t) dt + C(t_f). \quad (9.1)$$

The functions $u_1(t)$ and $u_2(t)$ represent the input of IL-2 and chemotherapy respectively. The functional J , the cost associated with a given treatment, is a sum of the amount of treatment given and the size of the tumor at the end of the treatment period. Additionally we can constrain $u_1(t)$ and $u_2(t)$ to remain within certain ranges. Finding the optimal treatment strategy is the equivalent of minimizing J . It will be important to choose the correct functional J and the appropriate constraints, but it is difficult to say

what exactly those are before we analyze the model. Although analytic methods for solving these problems exist, with such a large system as ours, it will probably be necessary to use computation.

The problem highlighted by this model, however, is the response of cytotoxic T-cells to the injection of IL-2. The next step is to make a model that looks at this process more closely. Due to the importance of timing in this problem, it may be necessary to use **delay differential equations**. These are differential equations where the derivative of the state variables at time t may depend on the value of the state variables at some earlier time. This may be necessary to model the timing of the release of IL-2 by cytotoxic T-cells as well as the proliferation of both cytotoxic and regulatory T-cells.

Bibliography

- [1] Alfonso R. M. Almeida, Bruno Zaragoza, and Antonio A. Freitas. Indexation as a novel mechanism of lymphocyte homeostasis: The number of cd4+cd25+ regulatory t cells is indexed to the number of il-2-producing cells. *Journal of Immunology*, 177:192–200, 2006.
- [2] Michael B. Atkins. Cytokine-based therapy and biochemotherapy for advanced melanoma. *Clinical Cancer Research*, 12:2353–2358, 2006.
- [3] Nicholas F. Britton. *Essential Mathematical Biology*. Springer, 2002.
- [4] Jorge Carneiro, Tiago Paixao, Dejan Milutinovic, Joao Sousa, Kalet Leona, Rui Gardner, and Jose Faro. Immunological self-tolerance: Lessons from mathematical modeling. *Journal of Computational and Applied Mathematics*, 184:77–100, 2004.
- [5] Craig Collins, Michael Daub, Renee Fister, Weiqing Gu, David Gross, James Moore, Lisette de Pillis, and Benjamin Preskill. Optimal control of immunotherapy and chemotherapy of tumors. unpublished.
- [6] Lisette de Pillis, Ami Radunskaya, and Weiqing Gu. Mixed immunotherapy and chemotherapy of tumor modeling, applications and biological interpretations. *Journal of Theoretical Biology*, 238:841–862, 2006.
- [7] Lisette de Pillis, Ami Radunskaya, and Charles Wiseman. A validated mathematical model of cell-mediated immune response to tumor growth. *Cancer Research*, 65:7950–7958, 2004.
- [8] Madhav V. Dhodapkar, Ralph M. Steinman, and Joseph Krasovsky. Antigen-specific inhibition of effector t-cell function in humans after injection of immature dendritic cells. *Journal of Experimental Medicine*, 193:233–238, 2001.

- [9] Madhav V. Dhodapkar, Ralph M. Steinman, Mark Sapp, and Hema Desai. Rapid generation of broad t-cell immunity in humans after a single injection of mature dendritic cells. *Journal of Clinical Investigation*, 104:173–180, 1999.
- [10] Renee Fister and Jennifer Hughes Donnelly. Immunotherapy: An optimal control theory approach. *Mathematical Biosciences and Engineering*, 2:499–510, 2005.
- [11] Avner Friedman. A hierarchy of cancer models and their mathematical challenges. *Discrete and Continuous Dynamical Systems-Series B*, 4:147–159, 2004.
- [12] Shea N. Gardner. A mechanistic, predictive model of dose-response curves for cell cycle phase-specific and -nonspecific drugs. *Cancer Research*, 60:1417–1425, 2000.
- [13] Arun T. Kamath, Sandrine Henri, Frank Battye, David F. Tough, and Ken Shortman. Developmental kinetics and lifespan of dendritic cells in mouse lymphoid organs. *Blood*, 100:1734–1741, 2002.
- [14] Denise Kirschner and John Panetta. Modeling immunotherapy of the tumor-immune interaction. *Journal of Mathematical Biology*, 37:235–252, 1998.
- [15] Kalet Leon, Agustin Lage, and Jorge Carneiro. Tolerance and immunity in a mathematical model of T-cell mediated suppression. *Journal of Theoretical Biology*, 225:107–126, 2003.
- [16] Howard A. Levine, Serdal Pamuk, Brian D. Sleeman, and Marit Nilsen-Hamilton. Mathematical modeling of capillary formation and development in tumor angiogenesis: Penetration into the stroma. *Bulletin of Mathematical Biology*, 63:801–863, 2001.
- [17] Burkhard Ludewig, Philippe Krebs, Tobias Junt, Helen Metters, Neville J. Ford, Roy M. Anderson, and Gennady Bocharov. Determining control parameters for dendritic cell-cytotoxic t lymphocyte interaction. *European Journal of Immunology*, 34:2407–2418, 2004.
- [18] D. G. Mallet and L. G. De Pillis. A cellular automata model of tumor-immune system interactions. *Journal of Theoretical Biology*, 239:334–350, 2006.

-
- [19] Markus Y. Mapara and Megan Sykes. Tolerance and cancer: Mechanisms of tumor evasion and strategies for breaking tolerance. *Journal of Clinical Oncology*, 22:1136–1151, 1996.
- [20] Joana Moreira and Andreas Deutsch. Cellular automaton models of tumor development: a critical review. *Advances in Complex Systems*, 5:247–267, 2002.
- [21] Brad Nelson. Il-2, regulatory T-cells, and tolerance. *Journal of Immunology*, 172:3983–3988, 2004.
- [22] Claes Ohlen, Michael Kalos, Laurence E. Cheng, Aaron C. Shur, Dole J. Hong, Bryan D. Carson, Niels C.T. Kokot, Cara G. Lerner, Blyth D Sather, Eric S. Huseby, and Philip D. Greenberg. Cd8+ t cell tolerance to a tumor associated antigen is maintained at the level of expansion rather than effector function. *Journal of Experimental Medicine*, 195:1407–1418, 2002.
- [23] Bill Purves, David Sadava, Gordon Orians, and Craig Heller. *Life: The Science of Biology*. Courier, 7 edition, 2004.
- [24] Yosef Refaeli, Luk Van Parijs, Cheryl London, Jurg Tschopp, and Abul Abbas. Biochemical mechanisms of IL-2-regulated, fas-mediated T-cell apoptosis. *Immunity*, 8:615–623, 1998.
- [25] American Cancer Society. Cancer facts and figures, 2006.
- [26] Ryan M. Teague, Blythe D. Sather, Jilian A. Sacks, Maria Z. Huang, Michell L Dossett, Junko Morimoto, Xiaoxio Tan, Susan E Sutton, Michael P Cooke, Claes Ohlen, and Philip D Greenberg. Interleukin-15 rescues tolerant CD8+ T-cells for use in adoptive immunotherapy of established tumors. *Nature Medicine*, 12:335–341, 2006.
- [27] Angela M. Thornton and Ethan M. Shevach. Suppressor effector function of CD4+CD25+ immunoregulatory T-cells is antigen nonspecific. *Journal of Immunology*, 164:183–190, 2000.
- [28] George Vlad, Raffaello Cortesini, and Nicole Suci-Foca. License to heal: Bidirectional interaction of antigen-specific regulatory T-cells and tolerogenic apc. *Journal of Immunology*, 174:5907–5914, 2005.
- [29] Theresa L. Whiteside. Immune suppression in cancer: Effects on immune cells, mechanisms and future therapeutic intervention. *Seminars in Cancer Biology*, 16:3–15, 2006.

Appendix A

Parameters

Parameter	Value	Death/Decay Rate Of	Source
ω	[.1, 1]	Immunogenic Dend. Cells	[13]
ω_C	$1.20 * 10^{-1}$	Cyto. T-Cells	[17]
ω_I	[.1, 1]	Immature Dend. Cells	[13]
ω_M	Not Set	Chemotherapy Medicine	Never Analyzed
ω_N	$1.0 * 10^{-2} g_2$	Naive T-Cells	[17]
ω_R	$1.0 * 10^{-2}$	Reg. T-Cells	Ad-Hoc Value
ω_T	[.1, 1]	Tolerogenic Dend. Cells	[13]
ω_2	[8, 33]	IL-2	[14]
ω_{10}	120	IL-10	Ad-Hoc Value

Table A.1: Death and Decay Rates. Units for all death and decay rates are days^{-1} .

Parameter	Value	Description	Explanation/Source
c	.018	Max Growth Rate of Tregs	[5]
γ	12	Growth Rate of Cytotoxic T-Cells	[17]

Table A.2: Other Growth Rates. Units for all growth rates are days^{-1} .

Parameter	Value	Description	Explanation/Source
c	.018	Max Growth Rate of Tregs	[5]
γ	12	Growth Rate of Cytotoxic T-Cells	Analysis
d_{CP}	60	Deactivation Rate of Cytotoxic T-Cells by Tregs	Analysis
d	Not Set	Deactivation Rate of Cytotoxic T-Cells by Dendritic Cells	[17]

Table A.3: Other Growth and Death Rates

Parameter	Value	Description	Explanation/Source
α_2	$.02\alpha_N$	Source Rate of IL-2	[5]
α_{10}	Not Set	Source Rate of IL-10 from Dendritic Cells	Never Analyzed
α_N	Not Set	Source Rate of Naive T-cells	Removed
a_T	Not Set	Activation Rate of Tolerogenic Dendritic Cells by Tregs	Never Analyzed
b_T	Not Set	Activation Rate of Tolerogenic Dendritic Cells by IL-10	Never Analyzed
a_{10}	Not Set	Source Rate of IL-10 from Tregs	Removed
a_C	Not Set	Activation Rate of Naive T-Cells by Dendritic Cells	Never Analyzed
a_{CP}	.462	Activation Rate of Cytotoxic Cells by IL-2	Analysis
a_R	Not Set	Activation Rate of Tregs	Removed
d	Not Set	Deactivation Rate of Cytotoxic T-Cells by Dendritic Cells	Never Analyzed
d_{CP}	60	Deactivation Rate of Cytotoxic T-Cells by Tregs	Analysis

Table A.4: Source, Activation and Deactivation Terms

Parameter	Value	Description	Explanation/Source
g_R	.018	Max Growth Rate of Tregs	[5]
g_2	12	Growth Rate of Cytotoxic T-Cells	Analysis
g_{10}	60	Deactivation Rate of Cytotoxic T-Cells by Tregs	Analysis

Table A.5: Levels of Half-Maximal Activation

Parameter	Description	Source
a_C	Activation Rate of Naive T-Cells by Dendritic Cells	[9]
α_{10}	Source Rate of IL-10	[8]
d_{CP}	Source Rate of Naive T-Cells	[8]
c	Activation Rate of Tregs Dendritic Cells by Cytotoxic T-Cells	[?]
K_X	Death Rate of Cell Population X due to Chemotherapy	[?]

Table A.6: Some parameters may be potentially be fit from the data found in the following sources

Parameter	Description	Value
k_C	Relative size of tumor needed for half maximal antigen stimulation	.02
k_R	Level of Tregs necessary for half maximal activation of tolerogenic dendritic cells	300
g_I	Maximum rate of T-cell activation by dendritic cells	20
g_T	Maximum rate of T-cell deletion by dendritic cells	2

Table A.7: Parameters of the Reduced System

Appendix B

Non-Dimensionalization

According to the **Buckingham-Pi Theory**, we can create rescaled model with fewer parameters and the same behavior. This process is called **non-dimensionalization** as the rescaled model doesn't have any units. The underlying principle is that the behavior of a system does not change depending on the units used.

$$\hat{t} = \omega_C t$$

$$\begin{aligned} \hat{T}_N &= \frac{\omega_C}{\alpha_N} T_N & \hat{T}_C &= \frac{a_2}{\omega_C g_2} T_C & \hat{T}_{CP} &= \frac{a_2 d_{CP}}{\omega_2 g_2 a_{CP}} T_{CP} \\ \hat{T}_R &= \frac{\alpha_{10} g_2 a_{CP}}{a_2 g_{10} d_{CP}} & T_R \hat{I}_2 &= \frac{I_2}{g_2} & \hat{I}_{10} &= \frac{I_{10}}{g_{10}} \\ \hat{\omega}_N &= \frac{\omega_N}{\omega_C g_2} & \hat{c} &= \frac{c}{\omega_C} & \hat{\omega}_R &= \frac{\omega_R}{\omega_C} \\ \hat{\omega}_{10} &= \frac{\omega_{10}}{\omega_C} & \hat{\gamma} &= \frac{\gamma}{\omega_C} & a_{\hat{CP}} &= \frac{a_{CP}}{\omega_C} \\ \hat{d}_{CP} &= \frac{d_{CP}}{\omega_C} & \hat{\omega}_2 &= \frac{\omega_2}{\omega_C} & \hat{\alpha}_2 &= \frac{\alpha_2 \alpha_N}{\omega_C g_2} \end{aligned}$$

Ommitting hats gives

$$\frac{dT_N}{dt} = 1 - \frac{\omega_N}{1 + I_2} T_N \quad (\text{B.1})$$

$$\frac{dT_C}{dt} = -a_{CP} \left(T_C \frac{I_2}{1 + I_2} - T_{CP} \frac{I_{10}}{1 + I_{10}} \right) - T_C \quad (\text{B.2})$$

$$\frac{dT_{CP}}{dt} = d_{CP} \left(T_C \frac{I_2}{1 + I_2} - T_{CP} \frac{I_{10}}{1 + I_{10}} \right) + \gamma T_{CP} \quad (\text{B.3})$$

$$\frac{dT_R}{dt} = c T_R \frac{I_2}{1 + I_2} - \omega_R T_R \quad (\text{B.4})$$

$$\frac{dI_2}{dt} = \alpha_2 T_N - \omega_2 I_2 + a_2 T_C \frac{I_2}{1 + I_2} \quad (\text{B.5})$$

$$\frac{dI_{10}}{dt} = T_R T_C - \omega_{10} I_{10}. \quad (\text{B.6})$$

B.1 Parameters

In the non-dimensionalized system, the parameters have no units but still have the same meaning as in the dimensionalized model.

Parameter	Value
ω_N	.1
ω_R	.1
ω_2	250
ω_{10}	1000
α_2	.5
c	.15
a_{CP}	.462
d_{CP}	500
γ	100

Table B.1: Parameters of Non-Dimensionalized Model